

Basics of Detailed Thermal-Hydraulic Model for Thermal Design of Oil Power Transformers

Zoran R. Radakovic and Marko S. Sorgic

Abstract—This paper presents the method for the calculation of temperatures inside oil power transformers, based on detailed thermal-hydraulic model. Starting from the construction of a transformer, physical parameters of applied materials, temperature of the outer cooling medium, and distribution of power losses, the calculation method delivers detailed distribution of temperatures: of the winding—in each conductor, of the oil—in each cooling channel and in each characteristic point, and in the core—on the surfaces and the hottest spots. The method is general [i.e., covers all oil circulation arts (ON, OF, and OD)]. Based on the method, the software for the thermal calculation of the majority of designs met in practice is developed.

Index Terms—Hot-spot factor, hot-spot temperature, thermal design, transformer.

I. INTRODUCTION

TEMPERATURES in oil power transformers represent the most important limiting factors for their loading. The highest temperatures of solid winding insulation (hot spot) and of the oil depend on loading conditions and have to be under certain limits. That is why the essential subject in the contract of delivery of the oil power transformer is temperature rise at the rated load—three values of temperature rises are specified: the hottest spot of solid winding insulation (hot spot) θ_{hs} , average winding temperature θ_{av} , and top oil θ_{to} [1].

It was always important to have accurate and reliable methods for thermal calculations of oil power transformers. It relates to transformer producers as well as to power utilities.

Producers have a strong interest that temperature rises of transformers come close to guaranteed temperature rises. If temperatures obtained in heat-run tests are lower than guaranteed, the transformer has, in fact, a higher rated power than sold. In other words, a producer could have used less material and made an additional profit on the transformer. This importance of accurate calculation of temperatures is especially high these days due to the rapid rise of the prices of materials in the last few years. These aspects can be very clearly expressed financially and understood on a management level [2].

From the other side, power utilities need good methods for transient calculations of temperatures for various technical issues: protection, monitoring, estimation of overloading capability, operational and strategic planning, etc.

Manuscript received September 08, 2008; revised August 01, 2009. First published January 15, 2010; current version published March 24, 2010. Paper no. TPWRD-00686-2008.

The authors are with the Faculty of Electrical Engineering, University of Belgrade, Belgrade 11000, Serbia (e-mail: radakovic@etf.rs; sorgic@etf.rs).

Digital Object Identifier 10.1109/TPWRD.2009.2033076

An important issue regarding temperature calculations is the value of hot-spot factor (H) used for the calculation of hot-spot temperature from values easily measured in heat-run tests. This factor cannot be calculated easily since it depends on the distribution of power losses, oil flows, and oil temperatures. As a matter of fact, the value of hot-spot temperature can only be determined by calculating detailed temperature distribution, which requires sophisticated models and software. If the producers do not have such calculation tools, it is necessary to measure the hot-spot temperature by means of using the fiber-optics measuring technique. This is explicitly recommended in a transformer loading guide [3].

The essential difference regarding methods which are used by transformer thermal design and methods used for temperature calculations during transformer utilization is that the models for the second ones can be parameterized by using the results of the heat-run test of produced transformers. Previous work of the first author was oriented to the calculation methods and thermal aspects in online operation of oil power transformers (for example, [4]). Of interest were transient thermal phenomena appearing in real loading conditions of variable load and outer cooling medium temperature. Basically, the model (i.e., the system of two nonlinear nonstationary mathematical equations) was used with the parameters of the model estimated from the results of heat-run test. Significant contributions to this topic are published in [5] and [6]. All of these methods were based on lumped model and none of them has really dealt with the hot-spot factor.

The only way to get the hot-spot factor is to calculate the detailed distribution of winding temperature (in each conductor) and to determine from them the hottest and the average winding temperatures. To achieve this, the proper approach is to build hydraulic and thermal networks with concentrated parameters. This model is described in this paper—the very basics can be found in [7]–[11]. According to extensive experience in this field, the authors would not recommend application of computational fluid dynamics (CFD) methods for the development of the tool for the thermal design of a complete transformer. The reasons are the problems of convergence and unreasonably long required computing time from the point of view of transformer design. From the other side, the classical approach in the industry of power transformers is to use simplified expressions for characteristic components (pressure drops and temperature differences) and to adjust coefficients in these expressions based on the results of heat-run tests. This approach has extreme limitations in accuracy and application to the cases exceeding previous practice. In addition, it is certain that the transformer producers do not have enough results of measurements with fiber optics to make any reliable and accurate estimation

of the hot-spot factor. Eventually, measuring results could be merged on a level of some international technical group—such opportunity is used in IEC, where the hot-spot factors for OFAF transformers are summarized in the Committee Draft version of IEC 60076-2. Nevertheless, no final recommendation for the simple determination of hot-spot factor is given; for the tested transformer of rated power in the range 63–1000 MVA, hot-spot factor changes in range from 1.29 to 2.01 (2.01 was the value for low-voltage winding, rated transformer power 605 MVA, Zig-Zag oil flow, where the average temperature rise was 11.9 K). If we were to apply a hot-spot factor of 1.3, the error in hot-spot temperature would be $(2.01-1.3) 11.7 \text{ K} = 8.3 \text{ K}$.

The developed calculation method delivers the exact value of the hot-spot factor and is consequently important not only for the design of the transformer, but also for the calculation methods used in real operating conditions; the hot-spot factor can be used in some other simpler calculation methods aimed to the calculation of temperatures in real operational conditions. This paper deals with the thermal model, while for the losses, it is assumed that they are known from the calculation of field and eddy losses (at a specified uniform temperature of the winding). We just recalculate them in an iterative procedure to the temperature of the specific conductor.

II. BASICS OF THERMAL-HYDRAULIC MODEL

Detailed THM is strictly based on the following: 1) the conservation of heat; 2) the conservation of mass; and 3) pressure equilibrium in closed loops. These principles are followed in the modeling of global oil circulation between parts of the transformer (winding, core, cooler, etc.) (i.e., determination of oil flow through them). They are also used by building hydraulic and thermal networks of individual parts of transformers, aimed for the calculation of distribution of oil flow in oil channels in these parts.

In this section, the very basics of the model are exposed. An introduction to THM is done through two simplified examples:

- the simplest single oil loop (winding and radiators);
- idealized transformer with two windings and the radiators.

A. Simplest Single Oil Loop

1) *Produced Pressure*: The oil circulation is caused by thermal and pump driving forces. The thermal driving force appears as the consequence of change of oil density [7]. Due to oil flow throughout the elements of the oil circulation path, the pressure drop appears. Both produced pressure and pressure drop and depend on oil flow. In steady-state oil flow, Q should have values so that the equilibrium of produced pressure and total pressure drop exists.

Fig. 1 shows a simple single oil loop. Oil is heated in the winding (AB), flows through the space above the winding (BC), is cooled in the radiator (CD), and flows through the space between the output from the radiators and the winding (DA). In the regions BC and DA, the heat exchange exists (for example, cooling on connecting tubes), but is negligible compared to the heat exchanged in windings and radiators; consequently, the change of oil temperature is also negligible in this region.

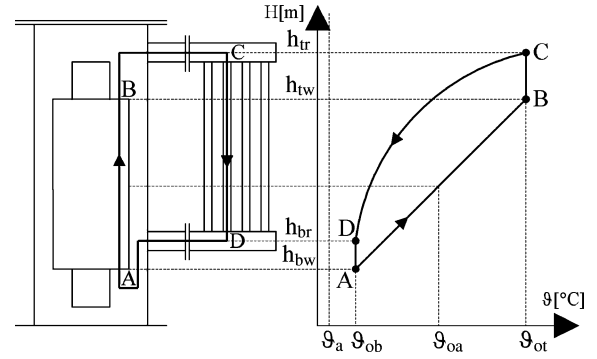


Fig. 1. Change of oil temperature along the simplest oil loop.

- ϑ_a ambient temperature ($^{\circ}\text{C}$);
- ϑ_{ob} bottom oil temperature ($^{\circ}\text{C}$);
- ϑ_{ot} top oil temperature ($^{\circ}\text{C}$);
- ϑ_{oa} average oil temperature ($^{\circ}\text{C}$).

The thermal driving force (p_T) is equal to the integral of the oil density along the oil loop

$$p_T = \oint \rho \vec{g} d\vec{l} = \oint \rho g \cos \varphi dl \quad (1)$$

- ρ oil density (kg/m^3);
- \vec{g} gravity vector (9.81 m/s^2);
- φ angle between velocity and gravity vector;
- \vec{l} path vector (in meters).

Fig. 2 shows the change of oil density along the oil loop. For simplified representation, convenient for basic understanding, (1) can be simplified [11] to the form

$$p_T = \rho_r g \beta \Delta\theta_{Ot} \Delta H \quad (2)$$

- ρ_r oil density at referent temperature (kg/m^3);
- β volume expansion coefficient of the oil ($1/^{\circ}\text{C}$);
- $\Delta\theta_{Ot}$ vertical temperature gradient ($\vartheta_{ot} - \vartheta_{ob}$) (in degrees Kelvin);
- ΔH height difference between the vertical center of the radiators and that of the winding (at this point, certain refinement is possible [7]) (in meters).

If there is the pump pumping oil directly to the windings (OD cooling), total produced pressure (p_{prod}) is equal to the sum of p_T and pressure produced by the pump (p_P), where p_P is much larger than p_T

$$p_{\text{prod}} = p_T + p_P \quad (3)$$

2) *Pressure Drop*: Pressure drop in the oil loops is equal to the sum of individual pressure drops in elements through which oil streams. There are two types of pressure drops:

- 1) dispersed pressure drop—flow through strait tubes of constant cross-sections;

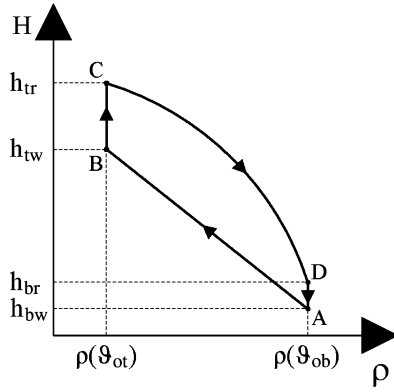


Fig. 2. Change of density of oil along the simplest oil loop.

2) local pressure drop—elements where oil changes oil streaming lines.

Standard form of the equations for pressure drop (Δp , in Pa) is

$$\Delta p = \xi \frac{\rho w^2}{2} \quad (4)$$

w oil velocity (in meters per second);
 ξ pressure drop coefficient.

Equations for calculating pressure drops coefficient ξ can be found in the literature, first of all in handbooks such as [12] and [13]. As an illustration, for the circular tube of diameter d (in meters) and length l (in meters), in the range of Reynolds number (Re) below 2000, ξ is calculated as

$$\xi = \frac{64 l}{Re d} \quad (5)$$

$$Re = \frac{wd}{\nu} \quad (6)$$

ν kinematic viscosity (m^2/s).

In handbooks, coefficients ξ can be found for different geometries—for example, oil splitting, oil joining, and corner (18 different basic elements are identified until now for hydraulic modeling of the transformer parts). At this point, it should be emphasized that the handbooks do not contain all formulas for coefficients ξ corresponding to cases of oil streaming met in transformers. This is one of the serious problems and subject of research by building exact detailed THM. There are two ways how to get these coefficients: experimentally (measurements on the models) and using CFD computations (the results are used to established formulas (or tables) for coefficients ξ).

The calculation of pressure drops is based on forming hydraulic networks. By proper programming, it is possible to automatically generate the structure of hydraulic networks (i.e., corresponding nonlinear equations) by using the input data about the type and geometry of the element (winding, for example—for more details, see Section III). For calculating elements of the networks, the corresponding formulas are used.

3) *Oil Temperatures and Equilibrium of Pressure*: From previously exposed text, it is clear how the pressure drop depends on oil flow. Oil flow also influences the value of produced

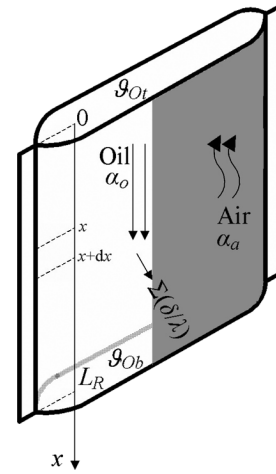


Fig. 3. Energy balance of oil in the radiator.

pressure, both the thermal driving force and pressure produced by the pump. This chapter describes the determination of the thermal driving force. From (1) and (2) and Figs. 1 and 2, it can be seen that the thermal driving force depends on the change of temperature along the oil circulation loop. The following energy balance is valid for the winding:

$$P_\gamma = \rho c_P Q (\vartheta_{ot} - \vartheta_{ob}) \quad (7)$$

P_γ power losses in winding (in Watts);
 ρ oil density at ϑ_{ob} (kg/m^3);
 c_P specific heat of the oil ($J/(kg K)$);
 Q oil volume flow (mm^3/s).

From (7), it is clear that the increase of oil flow leads to a decrease of temperature gradient ($\vartheta_{ot} - \vartheta_{ob}$) and the consequent decrease of the thermal driving force (2).

In order to calculate produced pressure using simplified (2), we need the temperature gradient ($\vartheta_{ot} - \vartheta_{ob}$). So far, we have two equations: 1) for the pressure equilibrium (3) and 2) energy balance (7), but three unknowns: flow (Q) and two oil temperatures (ϑ_{ot} and ϑ_{ob}). The third equation is the one describing the cooling on the radiator. The differential equation of energy balance (Fig. 3) of oil in the radiator is

$$k_P O (\vartheta_O(x) - \vartheta_a) dx = \rho c_P Q_O d\vartheta_O(x) \quad (8)$$

k_P total heat transfer coefficient (HTC) ($W/(m^2K)$);
 O circumference of outer radiator cross-section (in meters); for circular tube $O = \pi D$, where D is an outer diameter of tube;
 $\vartheta_O(x)$ oil temperature at position x ($^\circ C$);
 Q_O oil flow through the radiator (m^3/h).

The previous equation is similar to the well-known basic equation of heat exchangers [14], with the difference that the temperature of one of the fluids (in this case, the air) is constant.

The total HTC k_P can be taken as constant, for 1-D wall (this is a commonly used approach in a theory of heat exchangers, meaning that the high thermal resistance through the tube in the

direction of fluid flow causes low heat transfer through the tube in this direction), which is equal to

$$k_P = \frac{1}{\frac{1}{\alpha_O} + \sum \frac{\delta_{Ri}}{\lambda_{Ri}} + \frac{1}{\alpha_a}} \quad (9)$$

- α_O convection HTC from the oil to the radiator (W/(m²K));
- $\sum(\delta_{Ri}/\lambda_{Ri})$ sum of ratios thickness to thermal conductivity of radiator paintings layers and of the iron wall (W/(m²K));
- α_a convection HTC from the radiator to the air (W/(m²K)).

The constant value of α_O and α_a are taken as the average convection HTC over the surface of the radiator. This is acceptable approximation since in this case, convection HTC does not change over the radiator significantly—entry regions are small compared to the total length. Under this assumption, the solution of (8) is

$$\vartheta_O(x) = \vartheta_a + (\vartheta_{Ot} - \vartheta_a)e^{-\frac{k_P O}{\rho c_P Q} x} \quad (10)$$

By integrating cooling power along the radiator

$$P = \int_0^{L_R} (\vartheta_O(x) - \vartheta_a) k_P O dx \quad (11)$$

we get

$$P = \rho c_P Q (\vartheta_{Ot} - \vartheta_a) \left(1 - e^{-\frac{k_P O L_R}{\rho c_P Q}} \right) \quad (12)$$

Due to assumptions that there is no cooling on tank surfaces and no core losses, the power of heat transferred through the radiator is equal to power losses in the windings ($P = P_\gamma$). Consequently, from (12) and (7) and condition (3), two unknown temperatures and oil flow can be determined. Thermal driving force can be calculated using simplified (2) or exact (1), where real shape of temperature, defined by (10), is used. The determination of convection HTCs is discussed in Section II-C.

B. Simple Example of Two Windings and the Radiators

Fig. 4 shows a simple example of oil loops for the two winding case. The following assumption is made: only one phase exists, there is no core losses, there is no oil flow through the core, no cooling on tank surfaces, and no bypass of the oil (between the windings and the tank).

In the case from Fig. 1, the temperature of top oil has the value by which the cooling power on the radiators is equal to the power losses in the winding. For the case in Fig. 4, there is the oil mixture, and the corresponding mathematical model becomes more complicated.

1) *System of Equations for Oil Temperatures:* Let us suppose at the moment that the oil flows through winding 1 (Q_1) and through winding 2 (Q_2) are known; they will be obtained later as the result of the equilibrium of produced pressure

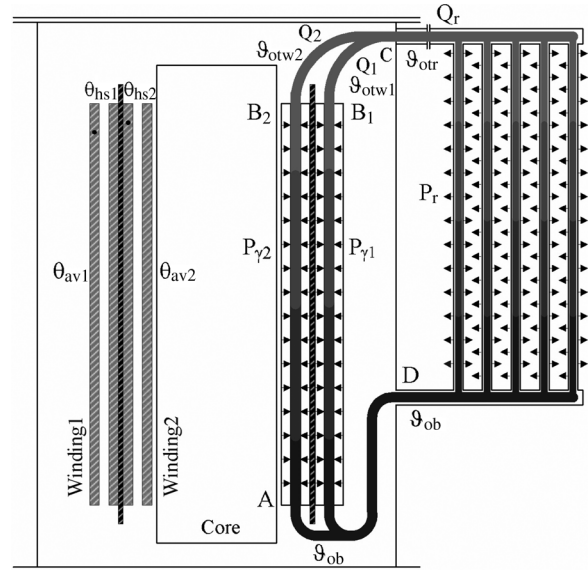


Fig. 4. Simplified example of oil flow in a transformer with two windings.

- ϑ_{Ob} bottom oil temperature (°C);
- ϑ_{otw1} oil temperature at the top of winding 1 (°C);
- ϑ_{otw2} oil temperature at the top of winding 2 (°C);
- ϑ_{otr} oil temperature at the top of radiators (°C);
- $P_{\gamma1}$ power losses in winding 1 (in watts);
- $P_{\gamma2}$ power losses in winding 2 (in watts);
- Q_1 oil flow through winding 1 (m³/s);
- Q_2 oil flow through winding 2 (m³/s);
- Q_r oil flow through radiators (m³/s);
- θ_{hs1} hot-spot temperature rise of winding 1 (in degrees Kelvin);
- θ_{hs2} hot-spot temperature rise of winding 2 (in degrees Kelvin);
- θ_{av1} average temperature rise of winding 1 (in degrees Kelvin);
- θ_{av2} average temperature rise of winding 2 (in degrees Kelvin).

and total pressure drop in two oil loops (one is formed by oil flowing through winding 1 and the radiators and another through winding 2 and the radiators). From the energy balance for both windings and for the radiators, the following equations can be written:

$$P_{\gamma1} = \rho c_P Q_1 (\vartheta_{otw1} - \vartheta_{Ob}) \quad (13)$$

$$P_{\gamma2} = \rho c_P Q_2 (\vartheta_{otw2} - \vartheta_{Ob}) \quad (14)$$

$$P_{\gamma1} + P_{\gamma2} = \rho c_P (Q_1 + Q_2) (\vartheta_{otr} - \vartheta_{Ob}) \quad (15)$$

- ρ oil density at ϑ_{Ob} (kg/m³);
- c_P specific heat of the oil (J/(kg K)).

Oil volume flows are related to the bottom oil temperature (mass flow is constant) whereas specific heat is taken at the average oil temperature $(\vartheta_{Ob} + \vartheta_{ot})/2$; for ϑ_{ot} , in (13) ϑ_{otw1} is taken, in (14) ϑ_{otw2} and in (15) ϑ_{otr} .

As in the case of the simplest single oil loop, the equation describing cooling on the radiator is needed. It is the same as (12), where the sum of oil flows Q_1 and Q_2 replaces Q , the sum of $P_{\gamma1}$ and $P_{\gamma2}$ replaces P , and ϑ_{otr} replaces ϑ_{ot} . The calculation procedure of four unknown temperatures and two flows is iterative: with assumed oil flows, first, the temperatures are calculated, and afterwards oil pressure components, followed by the check of pressure equilibrium. If pressure drop equilibrium

in one or both oil loops is not fulfilled, the oil flows are changed, and the calculation procedure of oil temperatures and pressures is repeated.

So the final results of the described procedure are oil flows through the windings and the radiators as well as oil temperatures at the inlet and outlet of these parts. Oil flow and inlet oil temperature are substantial input values for the calculation of distribution of temperatures in the windings.

2) *Splitting of Equations for Pressure Equilibrium*: There is an interesting alternative to the previously described procedure of equalizing produced pressure and total pressure drop in complete oil loops. The integral describing thermal driving force (1) can be split into two integrals—one corresponding to oil flow through the tank and one to oil flow through the radiators (if the pump exists, the pressure produced by the pump (p_{Pump}) is added to this second integral); for the loop related to winding 1 (Fig. 4), it yields

$$p_{prod} = \left(\int_{DAB_1C} \rho g \cos \phi ds \right) + \left(\int_{CD} \rho g \cos \phi ds + p_{Pump} \right). \quad (16)$$

Pressure drops (p_D) can be grouped into two sums: the first is the sum of pressure drops inside the tank, including winding 1— p_{DTank1} and the second in the radiators (including entrance and exit from them)— p_{DRad} . The pressure equilibrium equation

$$p_{prod} = p_{DTank1} + p_{DRad} \quad (17)$$

can be now written as

$$\left(\int_{CD} \rho \vec{g} d\vec{l} + p_{Pump} \right) - p_{DRad} = p_{DTank1} - \int_{DAB_1C} \rho \vec{g} d\vec{l}. \quad (18)$$

For winding 2, the corresponding equation yields

$$\left(\int_{CD} \rho \vec{g} d\vec{l} + p_{Pump} \right) - p_{DRad} = p_{DTank2} - \int_{DAB_2C} \rho \vec{g} d\vec{l}. \quad (19)$$

This splitting is quite an important principal and is used for forming the hydraulic networks of parts of a transformer. From (18) and (19), it is clear that the sum of gravitational components (terms of integrals of densities) and pressure drops in parallel branches between two points has to be the same. The systematic following of this principal simplifies and accelerates the needed calculation time for complex structures of transformer parts (Section III).

C. Thermal Resistance to Conduction and Convection

Heat transfer on each surface element of the transformer parts with the heat exchange can be described by simple expressions for thermal resistance (in Kelvin per watts), valid for 1-D heat transfer. This does not mean the models are 1-D (they are mainly 2-D); only the resistance, for axial surface or for radial surface, is taken as for 1-D heat transfer. Due to realistic dimensions (of the thickness of insulation comparing the dimensions of copper of the conductor, for example), the error is negligible.

Thermal resistance to heat conduction through the plane wall is

$$R_\lambda = \frac{1}{\lambda} \frac{\delta}{S} \quad (20)$$

- λ thermal conductivity of the wall (W/(m K));
- δ thickness of the wall (in meters);
- S surface through which the heat is transferred (m^2).

This simplest form is sufficient to describe cases of conduction heat transfer in oil transformers (thermal resistance is equal to the ratio of the difference of temperatures of boundary wall surfaces and transferred heat).

For the convection, the fundamental equation for the temperature gradient between the surface (ϑ_S) and the fluid (ϑ_f) by transferring the heat q through surface S to the fluid is

$$\vartheta_S - \vartheta_f = \frac{1}{\alpha S} q \quad (21)$$

- α convection HTC from surface to the fluid (W/(m^2K)).

The following convection heat transfers are of interest: from surfaces of active parts to attaching oil, from oil to surfaces of the cooling elements (radiators, compact coolers), from the cooling elements to outer cooling fluid (air, water). In the literature, there are equations for convection HTC for a certain number of configurations appearing in oil transformers, such as: 1) one-side heated channels; 2) both sides-heated channels (based on known fluid velocity: for the oil inside transformer and for the air by AF-cooled radiators); 3) both side-heated channels (for the air by AN-cooled radiators); 4) vertical wall (for the tank surface to oil and to the air side); 5) horizontal wall (four different variants—fluid under/above the wall, heat transferred to/from the fluid—used for tank and surfaces on the bottom and on the top of windings and core); and 6) inclined channels (for radial cooling channels without guiding oil).

As an illustration, the equation for convection HTC in the cooling channel will be given. Equations for “entry region” [14] can be applied (experience with the transformer data—the length of oil channels, the hydraulic diameters and oil velocities—points out that the streaming in oil channels in the windings is laminar and belongs to the “entry region”)

$$\alpha = \frac{\lambda N_{uD}}{D} \quad (22)$$

$$N_{uD} = 1.86 \left(\frac{Re_D Pr}{\frac{L}{D}} \right)^{\frac{1}{3}} \left(\frac{\mu}{\mu_S} \right)^{0.14} \quad (23)$$

- λ thermal conductivity of oil (W/(m K));
- N_{uD} Nusselt number;
- D hydraulic diameter of the tube (in meters) (it is equal to $4 S/O$; S —cross section of the oil channel, O is the circumference of the oil channel);

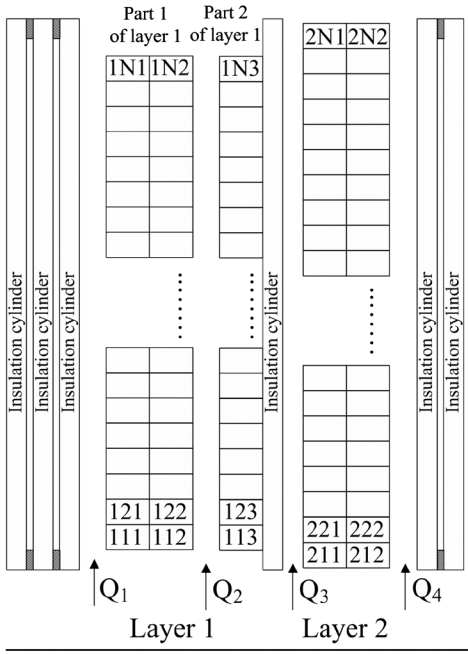


Fig. 5. Example of the layer winding with axial cooling channels.

- L length of the channel (in meters);
- Pr Prandtl number;
- μ dynamic viscosity of the oil at an average oil temperature (average oil temperature at the inlet and outlet of the channel) (Ns/m^2);
- μ_s dynamic viscosity of the oil at the surface temperature (Ns/m^2).

Similar to the pressure drop coefficient ξ , the accuracy of equations for α can be increased based on experiments on the models, based on CFD computations, but also based on the results of heat-run tests of transformers.

No radiation is treated (i.e., radiation heat transfer was neglected). The biggest relative impact it would have is by AN-cooled radiators, but it is also very small due to the small view factor between two facing plates forming the radiator. Only at the outer surface of the last plate of radiator radiation heat transfer would be comparable with the convection heat transfer to the air, but the effect to the cooling power of the complete radiator is small.

III. ILLUSTRATION OF FINE HYDRAULIC AND THERMAL NETWORKS OF THE WINDINGS

The majority of transformer parts represents the elements with complex geometry and complex oil flow and temperature distribution. Windings are the most complicated. As typical representatives, a layer winding with axial cooling channels formed with strips and disc winding with oil guiding elements—barriers (zig-zag flow) are considered in this section.

A. Layer Winding With Axial Cooling Channels

An example of this type of winding is shown in Fig. 5; the winding consists of two layers, each of them starting at a different distance from the bottom yoke. There are four axial cooling channels—two of them (1 and 4) are one-side heated

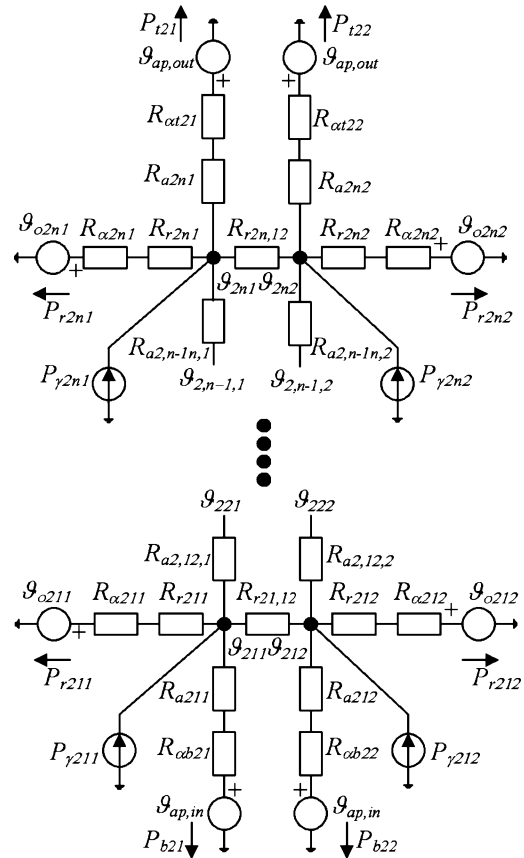


Fig. 6. Thermal network for part of the winding between cooling channels.

- P_γ power loss in each of the conductors (in watts);
- R_α thermal resistance to convection on axial surface of conductor (in degrees Kelvin per watt);
- R_{ob} thermal resistance to convection on bottom winding surface (in degrees Kelvin per watt);
- $R_{\alpha t}$ thermal resistance to convection on top winding surface (in degrees Kelvin per watt);
- R_r thermal resistance to conduction in radial direction; through single/double thickness of conductor insulation and eventual cylinder on layer surface (in degrees Kelvin per watt);
- R_a thermal resistance to conduction in the axial direction (in degrees Kelvin per watt);
- P_r power transferred to oil on the axial surface of the conductor (in watts);
- P_b power transferred to the oil on the bottom winding surface (in watts);
- P_t power transferred to the oil on the top winding surface (in watts).

and two of them (2 and 3) are both-side heated. Using equations from the convection heat-transfer theory (illustration: (22), (23), (6)), based on oil velocities, convection HTC's on the vertical surface of each conductor can be calculated. Different equations are used for one- and both- side heated channels. In addition, convection HTC's on the horizontal surfaces at the top and the bottom of the windings are calculated. For the winding from Fig. 5, three independent thermal networks are established—two for layer 1 and one for layer 2. In Fig. 6, the thermal network for layer 2 is shown. This network, as all other applied thermal and hydraulic networks, is 2-D (in the axial and radial direction). Local reduction of cooling, caused by any construction and production reasons, is not included in the following examples. We do not plan to extend the model into the third dimension, but to study this situation and to define the coefficients of ratio of maximum-to-average temperature

in such winding turns; if needed, the correction of the cooling surface of the turn will be introduced; the basic logic published in our paper [15] would be applied. Thermal resistances R_{α} , $R_{\alpha b}$, and $R_{\alpha t}$ are calculated by using the basic equation

$$R_{\text{Conv}} = \frac{1}{\alpha S} \quad (24)$$

α convection HTC ($\text{W}/(\text{m}^2\text{K})$);
 S conductor to the oil attaching surface (m^2).

Thermal resistances R_r and R_a are calculated using basic (20).

Based on the thermal circuit from Fig. 6, a system of linear equations can be written. Using mathematical methods of inverting sparse matrices, the temperature of each conductor can be determined. After that, the transferred heat to the oil (P_r, P_b, P_t) can be easily calculated.

Using (7), powers P_r and oil flows Q_3 and Q_4 , the temperature of oil in each cooling channel at each conductor 1 to N is calculated ($\vartheta_{O2i1}, \vartheta_{O2i2}, i = 1$ to n). More precisely, the channel with flow Q_3 is both side heated and the oil temperature also depends on P_r of part 2 of layer 1, for which the independent thermal circuit is used. The gravitational pressure drop in each of two cooling channels ($k = 1, 2$) is equal to

$$p_{gk} = g \int_0^H \rho(z) dz = g \sum_{i=1}^n (\rho(\vartheta_{O2ik}) H_i). \quad (25)$$

Similarly, frictional pressure drops are equal to

$$p_{fk} = \sum_{i=1}^N (\Delta p_{2ik}). \quad (26)$$

Δp_{2ik} is calculated by using (4)–(6), where density (ρ), kinematic viscosity (ν), and oil velocity (w) change along the cooling channels.

The total sum of pressures (the total gravitational + the total frictional + at the channel entrance, p_{in} + at the channel exit p_{out}), in the parallel channels is the same. They depend on flows Q_3 and Q_4 . The iterative procedure is implemented by changing the flows until reaching the equal total sum of pressures in both channels.

B. Disc Winding With Oil Guiding Elements

As an illustration, the section of the winding (two passes with four radial cooling channels per pass) is shown in Fig. 7. The hydraulic network of one pass is shown in Fig. 8 and the thermal network of one disc between radial cooling channels is in Fig. 9. In order to simplify the explanation, the case of one conductor in the axial direction between two radial cooling channels is shown and will be considered in further text. A reasonable simplification is made: it is assumed that the temperature of oil in all axial cooling channels on the entry oil side is the same (ϑ_{in}) as well as on the exit oil side (ϑ_{out}). It means that heat transfer from the conductor to oil in axial cooling channels is not taken into

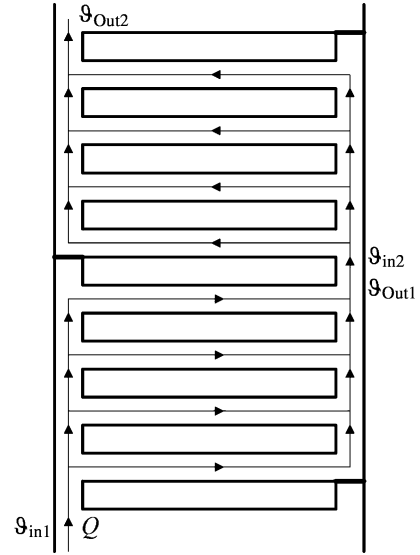


Fig. 7. Illustration of the disc winding with barriers.

ϑ_{in1} temperature of oil entering the first pass ($^{\circ}\text{C}$);
 ϑ_{out1} temperature of oil exiting the first pass ($^{\circ}\text{C}$);
 ϑ_{in2} temperature of oil entering the second pass ($^{\circ}\text{C}$);
 ϑ_{out2} temperature of oil exiting the second pass ($^{\circ}\text{C}$).

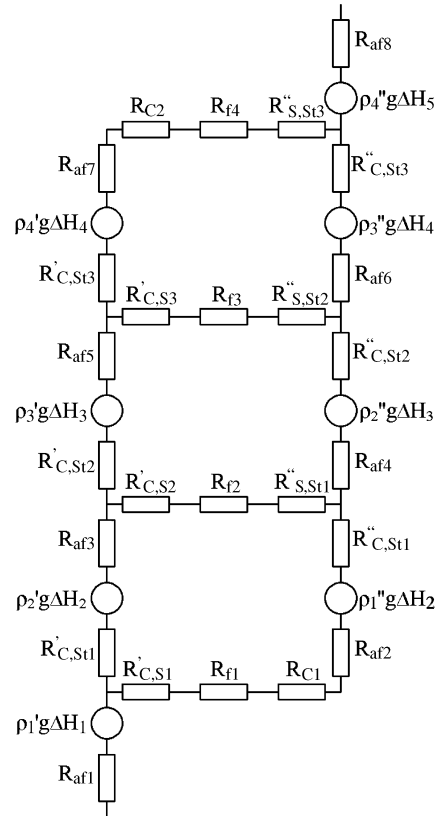


Fig. 8. Hydraulic network of one pass of disc winding with barriers.

account by determining the distribution of flow and temperature of oil. This simplification is acceptable since it does not noticeably influence neither elements for local pressure drops and for friction in Fig. 8 nor conductor temperature distribution. A great benefit is that nonlinear equations for calculating oil flows

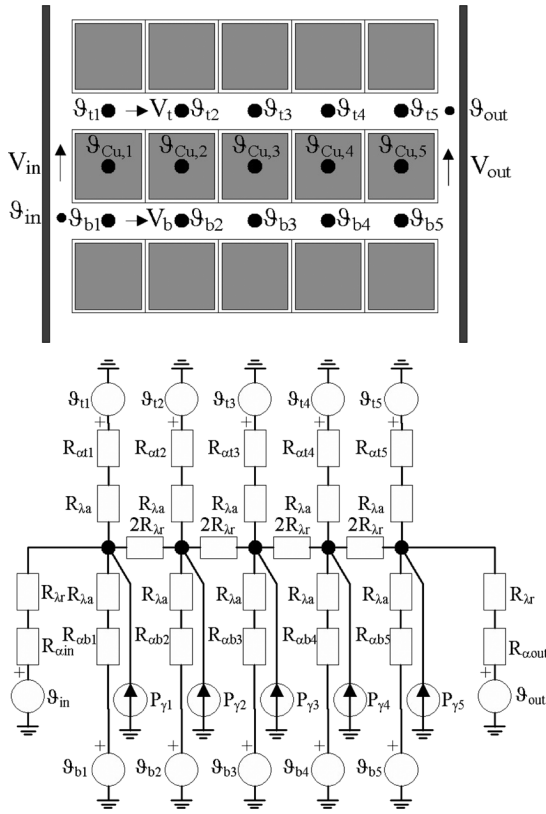


Fig. 9. Thermal network of one disc of disc winding with barriers.

through the channels and equations for calculating the temperature of conductors can be established and solved independently (first for flows and then for temperatures).

IV. STRUCTURAL TRANSFORMER PARTS AS ELEMENTS OF OIL LOOPS

A. Hydraulic Branches Inside Tank

This section relates to the pressure drop inside the tank ($p_{D\text{Tank}}$) for all cases excluding OD transformers containing also non-OD-cooled elements—core, or regulated windings, for example (the model is also developed for that case, but is rather complex and the description would be too extensive for this paper). The branches of oil flow separately for the windings and the core will be described in this section.

1) *Winding Elements:* In branches of oil flow through the windings, the pressure drops in the following elements exist:

- 1) oil distribution channel taking oil from the pipe coming from radiators and distributing oil to the holes under the windings; note: this pressure drop is averaged for the limbs since the difference of pressure drop for different limbs is negligible compared to total pressure drop;
- 2) oil-flow splitting, leaving the distribution channel and entering the hole under the winding;
- 3) friction (dispersed pressure drop) in holes under one or more windings; these holes are one of the elements used to adjust the oil-flow distribution between various windings;
- 4) oil channels or orifice for producing pressure drop which is added to pressure drop in holes (item C); these are also the elements for adjusting the distribution of oil flow.

- 5) the same as previous, but for single windings—for example, when more windings are supplied from one system of holes;
- 6) insulation system under the windings (from the point of view of hydraulic resistance (pressure drop), pressboard electrical insulation represents the complex system of oil channels);
- 7) winding itself (see Section III); in this zone, there is oil temperature and oil density change;
- 8) insulation system over the windings (similar to the system under the winding);
- 9) space under the pressing rings, through which the oil from different windings exits to free space in the tank.

Note: by ON- and OF-cooled transformers, elements 1)–5) usually do not exist.

2) *Core:* If the core is OD cooled (this is very difficult to implement in practice), 1)–4) in Sec. IV-A1) remain the same.

There are parallel oil flows through the parts of core. For example, with the three-limbs transformer, there are three equal oil flows through the zone of limbs and two equal oil flows in the zone of yoke between limbs. Oil temperature changes while oil flows through the cooling channels between sheets of the core. The total pressure drop between the point at the bottom (1) and the top of core (2) (height difference from 1 to 2 Z_3) for both oil paths, with flows Q_1 and Q_2 needing to be the same. It means that flows Q_1 and Q_2 have the values at which the following is valid (the orientation of gravity and path vector is opposite on the path 0– Z_3)

$$p_{D\text{Core}1} + \int_0^{Z_3} \rho_1(z)gdz = p_{D\text{Core}2} + \int_0^{Z_3} \rho_2(z)gdz. \quad (27)$$

$P_{D\text{Core}1}$ and $P_{D\text{Core}2}$ are frictional pressure drops due to flows Q_1 and Q_2 , respectively. In the zone of core window (Z_1, Z_2) of flow Q_2 , there is no frictional pressure drop. In this zone, there is no change of oil temperature and oil density. The oil distribution (i.e., the ratio Q_1/Q_2) strongly depends on power losses in yoke and limb, since oil temperatures and consequently densities and gravitational components of pressure drop strongly depend on power losses. Frictional pressure drops also depend on flows Q_1 and Q_2 : directly (pressure drop is proportional to the oil flow), but also via oil viscosity which is strongly dependent on the temperature [see (4)–(6)].

B. Hydraulic Elements Outside the Tank

Compared to the size and complexity of the hydraulic network inside the tank, the hydraulic network of elements outside the tank can be characterized as small and simple. It consists of pipes, valves, and radiators (or compact coolers) which, in a hydraulic sense, represent relatively long tubes of small diameter. There are different ways of connecting the radiators with the tank. With smaller transformers, they are mounted directly on the tank, with or without goose neck. Another possibility is to form radiator batteries and to connect them with tubes (pipes)—for cold oil and for hot oil—with the tank.

Again, a hydraulic network can be generated automatically by software from the given configuration, number, diameters, and lengths of piping for hot and cold oil, position and type of

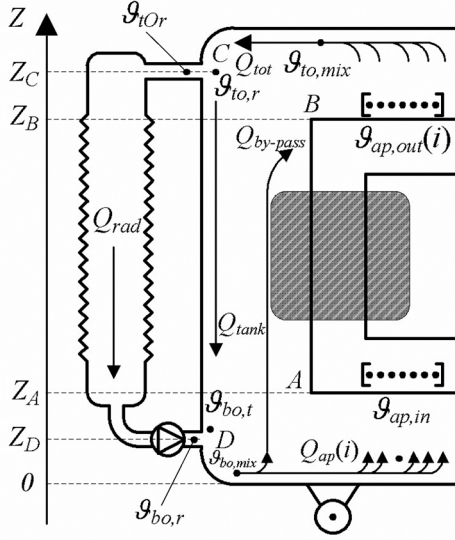


Fig. 10. Components of global oil flow for OF-cooled transformer.

- Q_{rad} oil flow through the radiators (compact cooler) (m^3/s);
- Q_{tank} oil flow downward the tank (m^3/s);
- $Q_{ap\ i}$ oil flow through each of active parts (windings and core) (m^3/s);
- Q_{bypass} oil flow in space between the windings and the tank (bypass of oil) (m^3/s);
- Q_{tot} total oil flow (m^3/s);
- $Q_{tot} = Q_{rad} + Q_{tank} = \sum(Q_{ap\ i}) + Q_{bypass}$;
- $\vartheta_{bo,r}$ temperature of oil exiting the radiators ($^{\circ}\text{C}$);
- $\vartheta_{bo,t}$ temperature of oil at the tank bottom ($^{\circ}\text{C}$);
- $\vartheta_{bo,mix}$ temperature of mixture of oils of temperatures $\vartheta_{bo,r}$ and $\vartheta_{bo,t}$ ($^{\circ}\text{C}$);
- $\vartheta_{ap,in}$ temperature of oil entering the active parts ($^{\circ}\text{C}$);
- $\vartheta_{ap,out\ i}$ Temperature of oil exiting each of active parts ($^{\circ}\text{C}$);
- $\vartheta_{to,mix}$ Temperature of mixed oils exiting active parts ($^{\circ}\text{C}$);
- $\vartheta_{to,r}$ Temperature of oil entering the radiators ($^{\circ}\text{C}$).

valves, number of bands, and data about the number of radiators, number of plates/tubes per radiator, and type and length of the plates/tubes (the alternative is data about the compact cooler). Heat exchange (i.e., change of oil temperature along the piping) does not need to be calculated since it is negligible.

C. Components of Oil Flow

On Fig. 10 realistic global oil-flow components are shown, for the sample transformer with OF cooling and for the case when the oil is cooled on the tank surface.

The case from Fig. 10, which is considered further on in the text, is just an illustration—the representation for OD cooling (i.e., its general case of existing OD- and non-OD-cooled active parts (windings and the core) is more complicated and will be exposed in future papers. Regarding oil flow near the tank wall surface, it can be downward (as shown in Fig. 10) or upward (it means that the oil is heated from tank walls—this occurs when the losses in tank walls due to stray flux are high). The algorithm determining if oil flows down—oil is cooled (calculated power from the oil to the tank P_{oil} positive $\Rightarrow Q_{tank}$ positive) or up—oil is heated (P_{oil} negative $\Rightarrow Q_{tank}$ negative), and afterwards calculating oil distribution in the zone between entrance and exit of oil from the radiators is developed.

The mathematical model contains several equations of energy balances for the oil; for example, for each active part, the equations connecting temperatures $\vartheta_{ap,in}$ and $\vartheta_{ap,out\ i}$ are analog

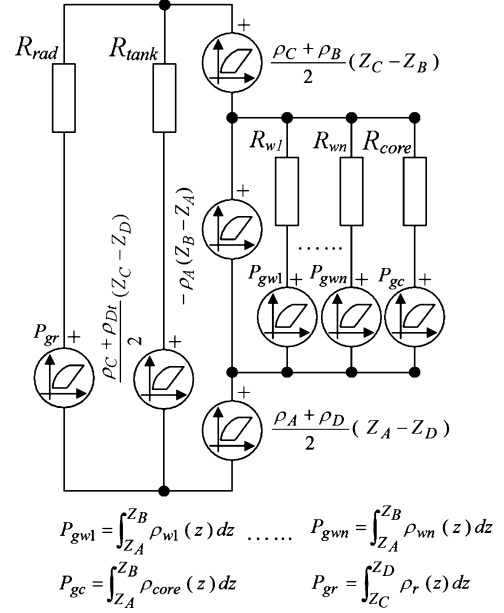


Fig. 11. Hydraulic network of the OF transformer with oil cooled on the tank surface.

- ρ_A is the oil density at temperature $\vartheta_{ap,in}$ ($^{\circ}\text{C}$) (kg/m^3);
- ρ_B oil density at temperature $\vartheta_{to,mix}$ ($^{\circ}\text{C}$) (kg/m^3);
- ρ_C oil density at temperature $\vartheta_{to,r}$ ($^{\circ}\text{C}$) (kg/m^3);
- ρ_{Dt} oil density at temperature $\vartheta_{bo,t}$ ($^{\circ}\text{C}$) (kg/m^3);
- ρ_D oil density at temperature $\vartheta_{bo,mix}$ ($^{\circ}\text{C}$) (kg/m^3);
- R_{wi} hydraulic resistance of the winding i , $i = 1$ to n ($\text{Pa}/(\text{m}^3/\text{s})$);
- R_{Core} hydraulic resistance of the core ($\text{Pa}/(\text{m}^3/\text{s})$);
- R_{rad} hydraulic resistance of the radiators ($\text{Pa}/(\text{m}^3/\text{s})$);
- R_{tank} hydraulic resistance corresponding to the friction in oil boundary layer near the tank surface ($\text{Pa}/(\text{m}^3/\text{s})$).

to (7). The oil mixture is also described by the corresponding simple equation. In addition to energy balance and oil mixture equations, the mathematical model contains equations of pressure equilibriums, corresponding to Fig. 11, where the complete hydraulic network is presented.

The values R_{wi} , $\int_{Z_A}^{Z_B} \rho_{wi}(z) dz$ (also R_{Core} , $\int_{Z_A}^{Z_B} \rho_{Core}(z) dz$) are calculated by solving complex nonlinear hydraulic and thermal equations for the windings/core and other components described previously in Section IV. The algorithm for the calculation of components of global oil flow (for OF cooling and oil cooled on tank walls, taken as an example throughout this section) is given in Fig. 12.

V. BRIEFLY ABOUT OTHER COMPONENTS OF COMPLETE CALCULATION METHOD

A. Heat Transfer From the Radiator Surface to the Air

In previous text, the focus was on oil circulation and heat transfer from conductor to oil. One of the components of the complete mathematical model is heat transferred through the radiators ((12)) (i.e., convection HTC from radiator to air (α_a in (9)). It strongly depends on nature of air flow—forced (AF) or natural (AN). For AF, α_a depends on air velocity. The developed mathematical model covers different types of radiators (plate or tubular), the presence and position of horizontally and vertically blowing fans, type of fans, arrangement of fans, length of radiators, etc. Also, different parts of radiators, for example,

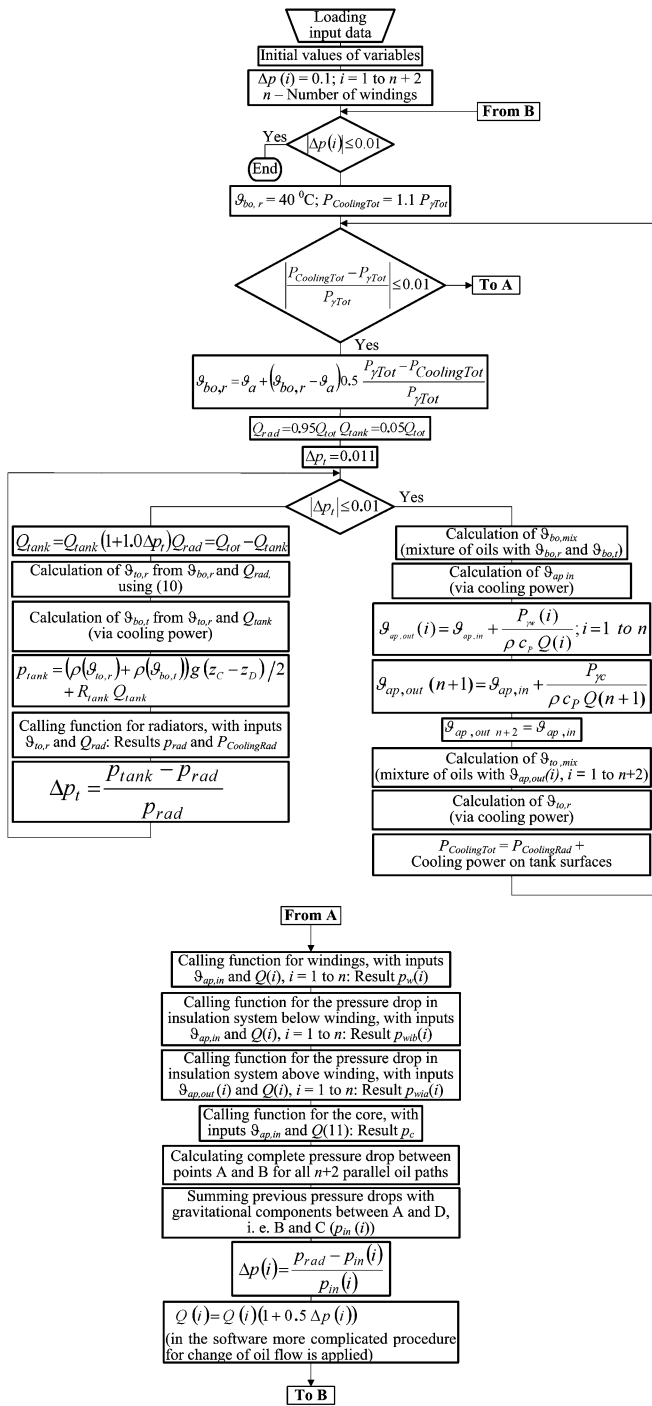


Fig. 12. Algorithm for the calculation of components of global oil flow.

AF- and AN-cooled (if exists) plates of radiators are identified and treated properly; the same is valid for characteristic sections along the length of plates/tubes of radiators—for example, AF- and AN-cooled sections by arrangement with horizontally blowing fans (radiators are positioned vertically).

Summing cooling powers on each part gives total cooling power on the radiators. Air flows (air velocities) are determined from the equilibrium of pressure produced by fans and pressure drop on the plates/tubes of radiators.

B. Models of Different Types of Windings

Models for the calculation of total pressure drop, distribution of oil velocity in cooling channels, and distributions of conductor and oil temperatures for the majority of windings met in practice (nine winding types—layer and disc, with different configuration of cooling channels, with and without barriers) are developed.

C. Insulation System of the Windings

There are two types of insulation pressboard elements.

The first one is between different windings: one or more cylinders with oil channels between them. If there is more than one cylinder, cylinders are sealed at the bottom (at least should be) and oil does not flow between the cylinders. It means that oil between cylinders has practically no influence on the cooling. More cylinders with blocked oil between can be considered adiabatic walls. If the sealing is not good, the oil flow between the cylinders can appear; this can jeopardize the cooling of the OD-cooled transformer and is one of the important quality issues in production.

The second type of pressboard elements appears between the windings and the yoke. This part, including also protection rings (potential rings) is designed by electrical insulation designer and from the point of view of cooling, it represents a labyrinth where pressure drop appears. The structure of insulation elements (type of rings: angle ring, double-angle ring, ring, type of protective ring: full or with opening, dimension of rings, oil channels and protective rings) is the input data for the calculation of pressure drop. The hydraulic network of insulation between bottom yoke and the bottom of the winding (i.e., between the top of the winding and top yoke) can be generated automatically by proper programming, while typical elements are being recognized (for example, angle ring to out after angle ring to in). A final result of solving the equations corresponding to the complete hydraulic network is a pressure drop in insulation below (above) the winding, while oil velocity in each channel is an intermediate result; the oil does not change temperature along this labyrinth.

D. Libraries of Elements

Hydraulic networks are built from basic elements. As mentioned in Section II-A2, there are 18 of these elements. By programming, it is convenient to organize the library of function for calculating pressure drops in basic elements. This library is opened for adding elements or improving the accuracy of calculation of pressure drop for existing elements.

It is also convenient to form the library of functions for convection HTC's for different geometries (see Section II-C).

Further convenient libraries are libraries with characteristics of equipment (pumps, fans, etc. of different suppliers).

VI. CALCULATED TEMPERATURES AND GUARANTEE TEMPERATURE VALUES

The result of the described method is a very detailed distribution of oil flow (global and inside the parts of transformer) and distribution of solid insulation and oil temperatures. Someone can say that such a detailed thermal picture of the transformer is not needed in practice. Nevertheless, due to nonuniform power

losses and oil velocities throughout the winding, it is the only way to accurately attain the critical (the highest) values of the temperatures, which are needed in practice.

In a standard heat-run test top oil, the average winding and winding hot-spot temperature rises are checked and have to be under guaranteed values. These values have to be forecasted in the design phase and it can be easily done from the obtained results of THM.

The hot-spot temperature is equal to the maximum conductor temperature. The average winding temperature is calculated through the dc resistance of the complete winding, with a sum of resistances of each turn (turn “*i*”), of cross-section S_i and diameter D_i at the calculated temperature of the turn ϑ_i

$$\vartheta_{avh} = \frac{\sum_i \frac{D_i}{S_i} (235 + \vartheta_i)}{\sum_i \frac{D_i}{S_i}} - 235. \quad (28)$$

From THM, it is clear that oil temperatures at the top of different windings are different; they also differ from oil temperature at the top of radiators. Consequently, the average oil temperatures in different windings are also different. In a standard heat-run test, the temperature gradient average winding minus average oil in radiators $\vartheta_{avh} - ((\vartheta_{to,mix} + \vartheta_{bo,r})/2)$ is practically considered as a temperature gradient winding to oil. So, temperature gradient winding to oil, which is measured in a standard heat-run test, is influenced not only on the conduction and convection heat transfer in the winding, but also on oil-flow distribution between the windings (see Fig. 10). According to this, the hot-spot factor obtained from THM and used to determine the hot-spot temperature from the results of heat-run test is equal to

$$H = \frac{\vartheta_{hs} - \vartheta_{to,mix}}{\vartheta_{av} - \frac{\vartheta_{to,mix} + \vartheta_{bo,r}}{2}}. \quad (29)$$

VII. NUMERICAL ILLUSTRATION

Due to limited space, only the illustration of the thermal calculation of winding (the one of type described in Section III-B.) is given. Further examples, case studies, and parametric studies of constructive transformer parts will be exposed in further publications. Fig. 13 shows the schematic of the winding with main data needed for the calculation.

Fig. 14 illustrates the distribution of total losses in each conductor (totally 92×5 conductors). Fig. 15 shows the calculated temperature distribution. The temperatures are dependent on distributed power losses, position of conductor node in the 2-D thermal network, position of the disc in the pass, position of the pass in the winding, and on local convection HTC on each conductor surface attaching the oil (they depend on oil velocity and conductor position). Although the losses reach the maximum at the first and second conductor of the discs, the temperatures reach the maximum at the third conductor, having the worst cooling conditions (radial temperature distribution in the hottest disc is shown in Fig. 16). As an interesting illustration, Fig. 17 shows the distribution of oil velocities in radial cooling

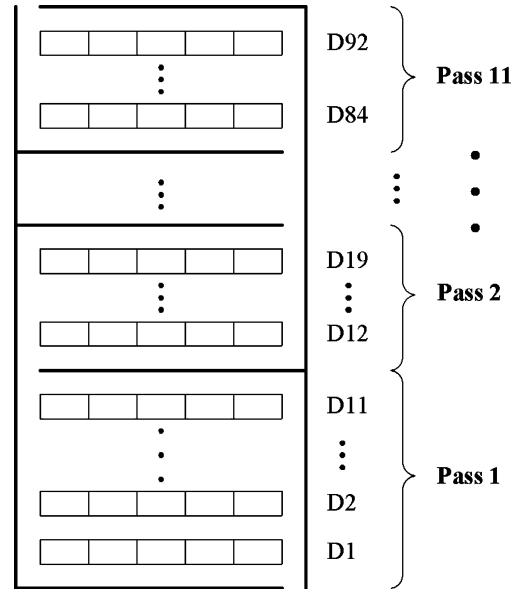


Fig. 13. Schematic of the winding.

Input data:

temperature of oil entering the winding $\vartheta_{bo} = 63$ °C;
total oil volume flow $Q = 47.2$ m³/h;
total losses $P_{\gamma Tot} = 123.35$ kW.

Data about passes:

pass 1: Discs D1 to D11, pass 2: Discs D12 to D19;
passes from 3 to 10 contain 8 discs and pass 11: D84 to D92.

Data about discs:

discs from D1–D26 and D67–D92 are made of conductor 2;
discs from D27–D66 are made of conductor 1.

Data about conductors:

height of conductor 1: 20.24 mm;
height of conductor 2: 18.74 mm;
width of both conductors: 14.9 mm;
thickness of paper insulation of both conductors: 2 mm.

Width of radial cooling channels:

below disks D1–D22 and D71–D92 and above D92: 5.5 mm;
below disks D23–D70: 4.6 mm.

Width of axial cooling channels:

from inner and from outer side: 5 mm.

channels of the pass 8 (with discs 60–67), where the hottest disc (D64) is situated in the middle. As shown in Fig. 17, the oil velocity has the lowest value in the middle of the pass, causing lower convection HTCs. Higher losses had a stronger effect and caused higher temperatures of conductors in pass 8 than higher oil temperatures (see Fig. 18) in pass 11.

The hot-spot temperature amounts to 96.42 °C, an average winding temperature of 87.61 °C, and a hot-spot factor of 1.29. The ratio of maximum losses in the conductor and average value of losses in conductors is 1.13, meaning nonuniformity of cooling contributed to a total hot-spot factor $1.29/1.13 = 1.14$. The hot-spot factor is kept on a relatively low level by increasing the cross section of the conductor at the top of the winding.

VIII. CONCLUSION

This paper deals with one of the topics of the highest importance in power transformer industry these days: the thermal design of oil power transformers. Accurate calculation reduces the

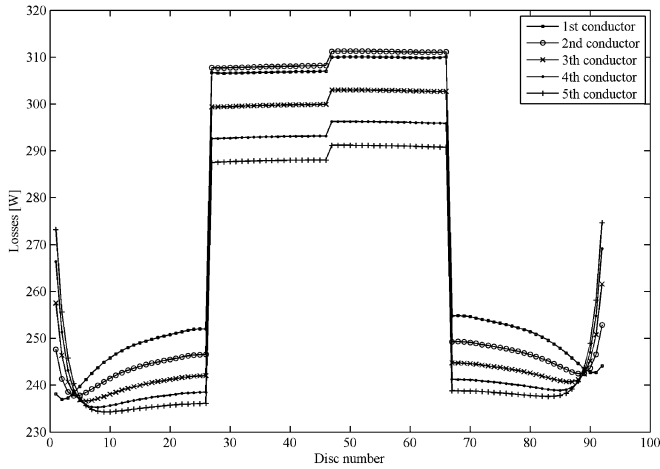


Fig. 14. Power losses distribution (conductor 1 is near the inner axial channel).

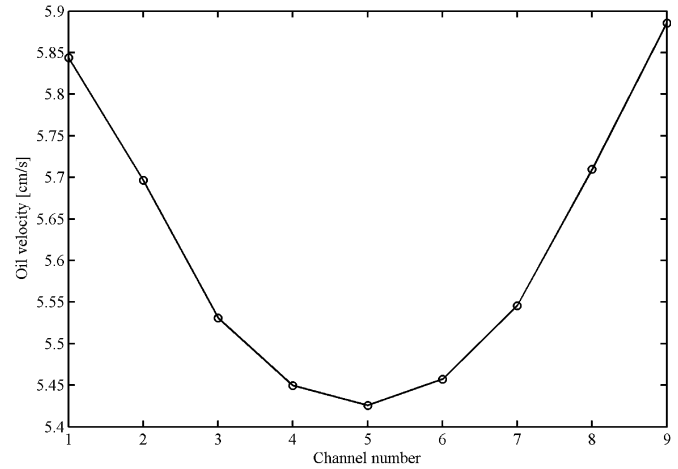


Fig. 17. Distribution of oil velocities in the radial channels of pass 8.

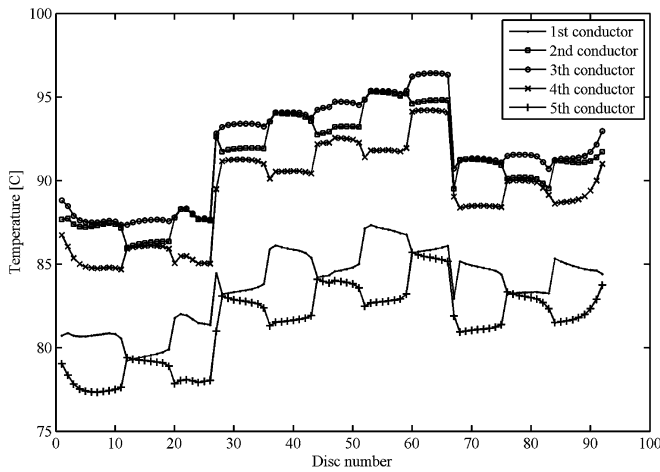


Fig. 15. Resulting temperature distribution.

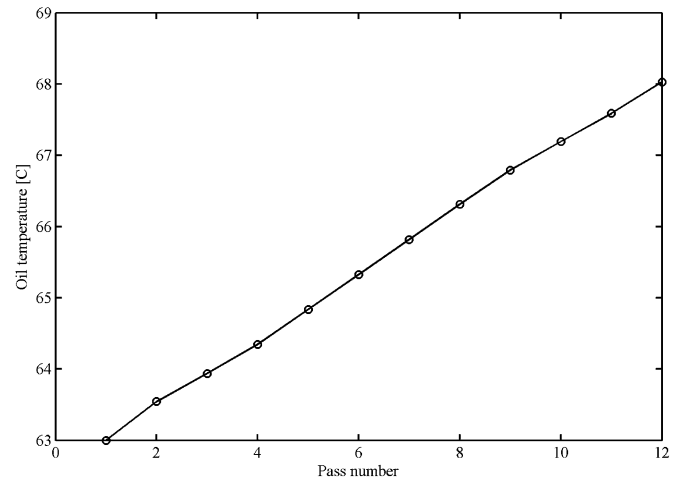


Fig. 18. Distribution of oil temperatures entering and exiting the passes.

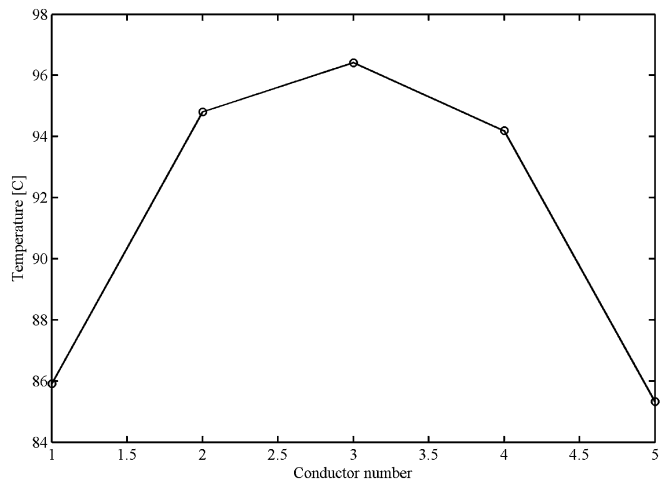


Fig. 16. Distribution of the temperatures in the hottest disc (disc 64).

calculation safety factors and significant savings of used material (copper, iron, oil, etc.) and a reduction of total production costs can be achieved. The aim of this paper is to expose the

basics of a general method for the thermal calculation of transformers, based on detailed THM.

The developed method and software are completely based on physics. The software covers the majority of constructions used in the production of oil power transformers, including relevant details. It is integrated (inner heating with outer cooling) and general (covers all cooling arts). Based on inputs, construction details (configuration, dimensions, and characteristics of material and built equipment) and values of power losses in each conductor, the software automatically generates complex hydraulic and thermal networks and solves them.

The final result of the method is a detailed distribution of oil flow throughout a transformer and a detailed distribution of oil and conductor temperatures. So the method delivers an exact value and position of the hot-spot temperature. This represents a crucial change in approach usually applied in practice (it is dominantly empirical) and an improvement in knowledge and methodology of the real estimation of hot-spot temperature.

Due to the complexity of physics and variety of construction solution, in this paper, it was not possible to deal with details.

The point was to describe and illustrate the methodology. Future publications will deal with interesting details, problems, and original solutions applied by transformer construction parts.

REFERENCES

- [1] *Power Transformers—Temperature Rise*, IEC Std. 60076-2, 1993.
- [2] Z. Radakovic and M. Sorgic, "Wirtschaftliche Betrachtung der thermischen Auslegung von ölgekühlten Leistungstransformatoren," *Elektrizitätswirtschaft*, pp. 32–38, 2008, Jg. 107, Heft 15.
- [3] *Power Transformers—Part 7: Loading Guide for Oil-Immersed Power Transformers*, IEC Std. 60076-7, Ed. 1.0, 2005-12.
- [4] Z. Radakovic and K. Feser, "A new method for the calculation of the hot-spot temperature in power transformers with ONAN cooling," *IEEE Trans. Power Del.*, vol. 18, no. 4, pp. 1284–1292, Oct. 2003.
- [5] L. W. Pierce, "An investigation of the thermal performance of an oil filled transformer winding," *IEEE Trans. Power Del.*, vol. 7, no. 3, pp. 1347–1358, Jul. 1992.
- [6] D. Susa and M. Lehtonen, "Dynamic thermal modeling of power transformers: Further development—Part II," *IEEE Trans. Power Del.*, vol. 21, no. 4, pp. 1971–1980, Oct. 2006.
- [7] K. Karsai, D. Kerényi, and L. Kiss, *Large Power Transformers*. New York: Elsevier, 1987.
- [8] A. J. Oliver, "Estimation of transformer winding temperatures and coolant flows using a general network method," *Proc. Inst. Elect. Eng., Pt. C*, vol. 127, pp. 395–405, 1980.
- [9] J. Zhang and X. Li, "Oil cooling for disk-type transformer windings—Part I: Theory and model development," *IEEE Trans. Power Del.*, vol. 21, no. 3, pp. 1318–1325, Jul. 2006.
- [10] J. Zhang and X. Li, "Oil cooling for disk-type transformer windings—Part II: Parametric studies of design parameters," *IEEE Trans. Power Del.*, vol. 21, no. 3, pp. 1326–1332, Jul. 2006.
- [11] M. Yamaguchi, T. Kumasaka, Y. Inui, and S. Ono, "The flow rate in a self-cooled transformer," *IEEE Trans. Power App. Syst.*, vol. PAS-100, no. 3, pp. 956–963, Mar. 1981.
- [12] I. E. Idelchik, *Handbook of Hydraulic Resistances*. Boca Raton, FL: CRC, 1994.

- [13] "VDI Wärmeatlas, Berechnungsblätter für den Wärmeübertragung," VDI-Gesellschaft Verfahrenstechnik und Chemieingenieurwesen (GVC), 1997.
- [14] F. P. Incropera and D. P. DeWitt, *Heat and Mass Transfer*, 5th ed. New York: Wiley, 2002.
- [15] Z. Radakovic, E. Cardillo, M. Schaefer, and K. Feser, "Design of the winding-bushing interconnections in large power transformers," *Elect. Eng. (Archiv Elektrotech.)*, vol. 88, pp. 183–190, 2005.



Zoran R. Radakovic was born in Belgrade, Serbia, on May 27, 1965. He received the B.Sc., M.Sc., and Ph.D. degrees in electrical engineering from the University of Belgrade in 1989, 1992, and 1997, respectively.

He was a Research and Teaching Assistant at the University of Belgrade; a Humboldt Research Fellow at the University of Stuttgart, Stuttgart, Germany; and Research and Development Engineer with Siemens AG, responsible for the development of cooling in the Technology and Innovation Department of the Transformer Division. Currently, he is a Professor with the Faculty of Electrical Engineering, University of Belgrade. Most of his career was in the field of thermal problems by power transformers. His other technical fields of experience are automatic digital control, power quality, grounding systems, electrical heating, and electrical installations. His main technical development is the modern software tool for the thermal design of power transformers.



Marko S. Sorgic was born in Pula, Croatia, on November 7, 1980. He received the Electrical Engineering degree from the University of Belgrade in 2006.

He is a Research and Teaching Assistant at the Faculty of Electrical Engineering, University of Belgrade, Belgrade, Serbia. Currently, he is working on research-and-development projects for the industry and ministry of science related to thermal problems by oil power transformers, power converters for solar panels, and the detection of electric arc.